

Investigating the interaction of x-ray free electron laser radiation with grating structure

Jérôme Gaudin,^{1,*} Cigdem Ozkan,¹ Jaromír Chalupský,² Saša Bajt,³ Tomáš Burian,² Luděk Vyšín,²
 Nicola Coppola,¹ Shafagh Dastjani Farahani,¹ Henry N. Chapman,³ Germano Galasso,¹
 Věra Hájková,² Marion Harmand,⁴ Libor Juha,² Marek Jurek,⁵ Rolf A. Loch,⁶
 Stefan Möller,⁷ Mitsuru Nagasono,⁸ Michael Störmer,⁹ Harald Sinn,¹
 Karel Saksl,¹⁰ Ryszard Sobierajski,⁵ Joachim Schulz,^{1,3}
 Pavol Sovak,¹¹ Sven Toleikis,⁴ Kai Tiedtke,⁴
 Thomas Tschentscher,¹ and Jacek Krzywinski⁷

¹European XFEL GmbH, Albert-Einstein-Ring 19, Hamburg, D-22671, Germany

²Institute of Physics, Academy of Sciences of the Czech Republic, Na Slovance 2, Prague 8, 182 21, Czech Republic

³Center for Free-Electron Laser Science, DESY, Notkestr. 85 Hamburg, D-22607, Germany

⁴HASYLAB/DESY, Notkestr. 85 Hamburg, D-22607, Germany

⁵Institute of Physics, Polish Academy of Sciences, Al. Lotników 32/46, Warsaw, PL-02-668, Poland

⁶Dutch Institute for Fundamental Energy Research, P.O. Box 1207, 3430 BE Nieuwegein, The Netherlands

⁷SLAC National Accelerator Laboratory, 2575 Sand Hill Road, Menlo Park, California 94025, USA

⁸RIKEN/SPring-8 Kouto 1-1-1, Sayo, Hyogo, 679-5148 Japan

⁹Helmholtz Zentrum Geesthacht, Institute of Materials Research, Max-Planck Str. 1, D-21502 Geesthacht, Germany

¹⁰Institute of Materials Research, Slovak Academy of Sciences, 04001 Kosice, Slovak Republic

¹¹Institut of Physics, P. J. Šafárik University, Park Angelinum, 04154 Kosice, Slovak Republic

*Corresponding author: jerome.gaudin@xfel.eu

Received April 23, 2012; revised May 31, 2012; accepted May 31, 2012;
 posted June 1, 2012 (Doc. ID 167189); published July 16, 2012

The interaction of free electron laser pulses with grating structure is investigated using 4.6 ± 0.1 nm radiation at the FLASH facility in Hamburg. For fluences above 63.7 ± 8.7 mJ/cm², the interaction triggers a damage process starting at the edge of the grating structure as evidenced by optical and atomic force microscopy. Simulations based on solution of the Helmholtz equation demonstrate an enhancement of the electric field intensity distribution at the edge of the grating structure. A procedure is finally deduced to evaluate damage threshold. © 2012 Optical Society of America

OCIS codes: 340.7480, 140.2600, 050.0050, 350.1820.

X-ray free electron lasers (XFELs) have demonstrated to be powerful tools for new, high impact research in different scientific fields. Motivated by successful experiments, new facilities (European XFEL, FLASH 2, LCLS 2) with improved properties in terms of energy per pulse over an extended wavelength range are currently under construction. Certain schemes promise to deliver up to tens of millijoule pulses. Soft x-ray spectroscopy experiments require monochromatized light, which can be provided through a grating-based monochromator. State-of-the-art x-ray grating is currently limited to length around 250 mm, resulting in quite high fluence impinging on the grating's surface. Damage of the grating is a major concern for the design of the beamline. Investigating and understanding the damage mechanism of grating structures is thus of fundamental importance for the development of the next generation XFELs. Predicting the damage threshold is difficult in the case of periodically structured surfaces, like gratings, as the electric field intensity distribution is highly nonhomogeneous at the surface and can lead to an enhanced damage mechanism as evidenced in the optical domain [1]. In this Letter, we report on both experimental and theoretical investigations of XFEL radiation interaction with grating structure.

The experiment was performed at the FLASH facility in Hamburg [2]. The sample was placed, under vacuum, in

the focus of a 2 m focal length mirror. The pulse duration was in the 80–150 fs range, and the radiation wavelength was measured to be 4.6 ± 0.1 nm. This error bar corresponds to the uncertainty on the absolute value of the wavelength and not to the pulse to pulse jittering, which has also been measured and found to be negligible ($\sim 1e-3$ nm). The beam was impinging the sample at the grazing angle $\alpha = 2^\circ \pm 0.1$, following a procedure described in [3]. The 200 V/mm (5 μ m periods) grating sample was produced by ion etching of a 1 mm thick Si wafer, with a duty ratio of 0.4. The groove depth was measured to be 13.5 nm. These parameters reproduce a real grating currently used in the Soft X-Ray beamline at the Linac Coherent Light Source (LCLS) [4]. The etched wafer was then coated with 45 nm of amorphous carbon (a-C), which is a typical coating for XFEL optics. Atomic force microscopy (AFM) measurement confirms that the coating exactly reproduces the ion etched profile. The grating sample, as well as a mirrorlike flat sample also made of 45 nm thick a-C coated on Si substrate, was exposed to single pulses with varying pulse energy. For each pulse, the pulse energy was measured with a gas detector monitor. The pulse energy monitor was located upstream from all optical components; e.g., the beamline transmission should be evaluated so the real pulse energy impinging on the sample can be known. As already stated, the radiation's wavelength was known

with an accuracy of ± 0.1 nm. The beamline consists of two plane Ni coated mirrors and three (2 plane+1 ellipsoidal) a-C coated mirrors (grazing incidence at 2 and 3 deg, respectively). In this wavelength domain, the beamline transmission is evaluated, taking into account the mirrors setting, to range from 0.20 (at 4.50 nm) to 0.46 (at 4.70 nm). This large variation is primarily due to the two upstream carbon coated mirrors present in the beamline, which are very sensitive around the carbon K-edge (at 4.37 nm). In this analysis, we assume therefore a wavelength of 4.60 nm corresponding to a beamline transmission of 0.39.

The exposed samples were analyzed *ex situ* by optical differential interference contrast (DIC) microscopy, which is sensitive to variations of optical refractive index, hence to any phase change, evidenced by a change of color. For each irradiated sample region, the area showing a color change (encircled areas shown in Fig. 1) in the microscope image was measured. For both the flat and the grating sample, the energy damage threshold (E_{th}) was determined by plotting the damaged area versus pulse energy, as shown in Fig. 2. Due to the non-Gaussian shape of the beam, only the very first data points should be fitted, as described in [5]. A line fit through the point gives a threshold for grating $E_{th}^G = 0.40 \pm 0.04 \mu\text{J}$ and $E_{th}^M = 1.17 \pm 0.16 \mu\text{J}$ for the flat sample. The error bars correspond to the confidence on the fit, at the 4.60 nm wavelength. We then calculate the ratio $E_{th}^M/E_{th}^G = 2.92 \pm 0.69$, which will be used for comparison with the model later, and is independent of the beamline transmission value.

The damage fluence threshold (F_{th}) is retrieved from the values of E_{th} and by making the following assumption. The beam profile was carefully characterized using imprints in the PMMA sample and following the procedure described in [5]. The effective area is found to be $A_{eff} = 22 \pm 2 \mu\text{m}^2$. We assumed that the beam footprint in case of grazing incidence is equal to the projected area, e.g., $A_{eff}/\sin(2)$. We obtained $F_{th}^G = 63.7 \pm 8.7 \text{ mJ}/\text{cm}^2$

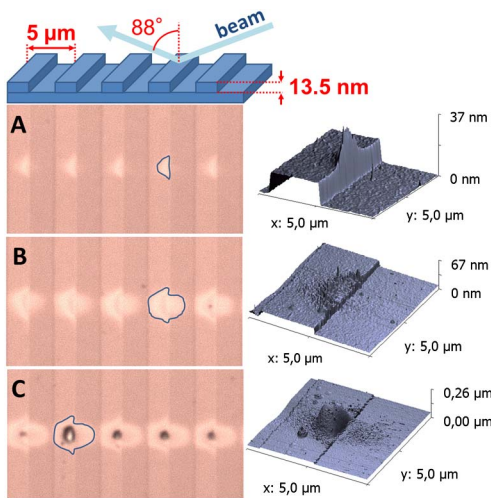


Fig. 1. (Color online) Top: schematic of the interaction of the experiment. Below: DIC microscopy (left) and AFM (right) measurements for three different fluences 356 (A), 806 (B), and 1115 mJ/cm^2 (C).

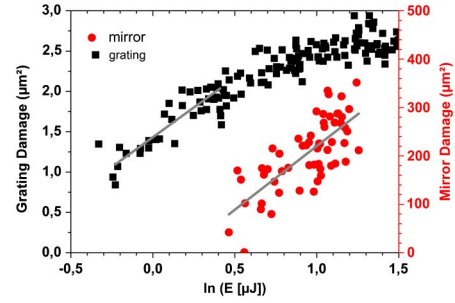


Fig. 2. (Color online) Damaged area on flat mirrorlike sample (red dots, right vertical scale) and grating (black square, left vertical scale).

for the grating and $F_{th}^M = 186.6 \pm 29.9 \text{ mJ}/\text{cm}^2$ for the flat sample.

Figure 1A, obtained with DIC microscopy, shows the onset of the damage on the edge of the grating structure. The AFM measurements confirm this observation, and show the extension of the damage first on the top of the groove as the fluence is increasing. The damage in the bottom part of the grating structure happens at higher fluence, as can be seen in Fig. 1B. At the highest fluence values (see Fig. 1C), black dots become visible due to the complete removal of the a-C coating and melting of the Si substrate.

To gain deeper insight in the understanding of the beam-grating interaction, an accurate model has to be used. As stated in the introduction, the electric field distribution at the surface of a grating can be highly non-homogeneous, especially while dealing with a coherent laser beam. We simulated the deposited energy distribution in the grating by solving the Helmholtz equation in a paraxial approximation. Assuming that the refractive index of the medium is nearly equal to 1 (which is true for the photon energy considered here), then the propagation of the scalar field ψ can be expressed as

$$\frac{\partial \Psi(\hat{r}, \hat{z})}{\partial \hat{z}} = \frac{i}{2} \cdot \frac{\partial^2 \Psi(\hat{r}, \hat{z})}{\partial \hat{r}^2} + \delta \varepsilon(\hat{r}, \hat{z}) \cdot \Psi(\hat{r}, \hat{z}), \quad \hat{r} = rk, \quad (1)$$

$$r^2 = x^2 + y^2, \quad \hat{z} = zk, \quad k = 2 \cdot \pi/\lambda.$$

λ is the wavelength, and $\delta(r, z)$ describes the difference between the dielectric constant of vacuum and the medium. The mathematical form of the Eq. (1) is identical to the time dependent, two-dimensional (2D) Schrödinger equation. Many effective methods exist to solve this type of equation; we chose a version of the beam propagation method that applies a split operator technique [6,7]. The grating is modelled by considering a 45 nm thick layer of a-C on Si-substrate. The grating profile used in the simulations as a boundary is the real profile measured with AFM. As a result, the model also takes into account possible effect of the microroughness. The real and imaginary part of $\delta(r, z)$ were taken from the Center for X-Ray Optics database [8]. We used a Gaussian beam profile as the initial condition. The incident angle and the photon energy were the same as in the experiment. The evolution of $|\psi(r, z)|^2$ is shown in Fig. 3. A standing wave builds up close to the grating's surface. The inset in Fig. 3 depicts the distribution of the absorbed energy in the

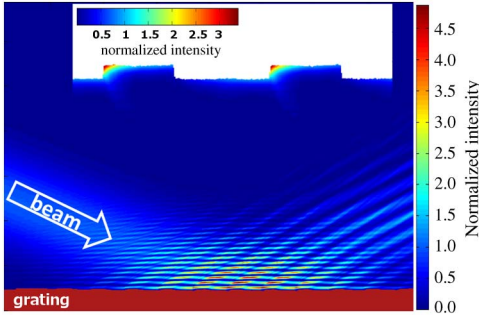


Fig. 3. (Color online) X-ray intensity distribution $|\psi(r, z)|^2$ close to the grating surface. The beam comes from the left. Inset: energy distribution absorbed in the grating. Both color scales are normalized intensity to the impinging beam.

grating's structure. The maximum absorption is taking place at the edge of the grating structure where the onset of damage is experimentally observed. Interestingly, microroughness does not increase the maximum of absorbed energy by more than few percent, as was confirmed by simulations on a smooth surface. Moreover, similar simulations (not shown) were also performed with a mirrorlike flat surface. The ratio of the maximum energy absorbed in the grating to the absorbed energy in the flat mirror is found to be $\gamma = 3.37$; γ can be directly related to the ratio of the damage thresholds. Both values agree, within the error bar of the experiment, demonstrating the quantitative accuracy of our approach. One should underline that γ does not reflect an enhancement of the intrinsic absorption process, but the nonhomogeneous field distribution at the surface of a grating leading to local enhancement of the absorbed energy.

In conclusion, we have investigated the interaction of 4.60 nm XFEL radiation with grating structure. An accurate description based on the Helmholtz equation shows that the specific field distribution at the surface leads to an enhancement of the absorbed energy at the edge of the laminar grating structure. The model provides a good qualitative and quantitative description of the experimental results. From a practical point of view, when designing a soft x-ray monochromator for an XFEL beamline, it is crucial to consider the fluence damage threshold values. We propose to first extrapolate $F_{\text{th}}^M(\alpha)$ for a flat mirrorlike surface using published data (for example, [3]). Next, simulations should be performed taking into account the exact geometry of the grating, to obtain γ . Finally the damage threshold on grating is deduced from the relation $F_{\text{th}}^G(\alpha) = F_{\text{th}}^M(\alpha)\gamma$.

This work was financially supported by the Czech Science Foundation (projects P108/11/1312, P205/11/0571, and P208/10/2302) and the Czech Ministry of Education (projects CZ.1.05/1.1.00/483/02.0061, CZ.1.07/2.3.00/483/20.0087, LA08024, and ME10046).

References

1. S. Hocquet, J. Neauport, and N. Bonod, *Appl. Phys. Lett.* **99**, 061101 (2011).
2. W. Ackermann, G. Asova, V. Ayvazyan, A. Azima, N. Baboi, J. Bähr, V. Balandin, B. Beutner, A. Brandt, A. Bolzmann, R. Brinkmann, O. I. Brovko, M. Castellano, P. Castro, L. Catani, E. Chiadroni, S. Choroba, A. Cianchi, T. Costello, D. Cubaynes, J. Dardis, W. Decking, H. Delsim-Hashemi, A. Delsierieys, G. Di Pirro, M. Dohlus, S. Düsterer, A. Eckhardt, T. Edwards, B. Faatz, J. Feldhaus, K. Flöttmann, J. Frisch, L. Fröhlich, T. Garvey, U. Gensch, Ch. Gerth, M. Görler, N. Golubeva, H.-J. Grabosch, M. Grecki, O. Grimm, K. Hacker, U. Hahn, J. H. Han, K. Honkavaara, T. Hott, M. Hüning, Y. Ivanisenko, E. Jaeschke, W. Jalmuzna, T. Jezynski, R. Kammering, V. Katalev, K. Kavanagh, E. T. Kennedy, S. Khodyachykh, K. Klose, V. Kocharyan, M. Körfer, M. Kollwe, W. Koprek, S. Korepanov, D. Kostin, M. Krassilnikov, G. Kube, M. Kuhlmann, C. L. S. Lewis, L. Lilje, T. Limberg, D. Lipka, F. Lühl, H. Luna, M. Luong, M. Martins, M. Meyer, P. Michelato, V. Miltchev, W. D. Möller, L. Monaco, W. F. O. Müller, O. Napieralski, O. Napoly, P. Nicolosi, D. Nölle, T. Nuñez, A. Oppelt, C. Pagani, R. Paparella, N. Pchalek, J. Pedregosa-Gutierrez, B. Petersen, B. Petrosyan, G. Petrosyan, L. Petrosyan, J. Pflüger, E. Plönjes, L. Poletto, K. Pozniak, E. Prat, D. Proch, P. Pucyk, P. Radcliffe, H. Redlin, K. Rehlich, M. Richter, M. Roehrs, J. Roensch, R. Romaniuk, M. Ross, J. Rossbach, V. Rybnikov, M. Sachwitz, E. L. Saldin, W. Sandner, H. Schlarb, B. Schmidt, M. Schmitz, P. Schmüser, R. Schneider, A. Schneidmiller, S. Schnepp, S. Schreiber, M. Seidel, D. Sertore, V. Shabunov, C. Simon, S. Simrock, E. Sombrowski, A. Sorokin, P. Spanknebel, R. Spesyvtsev, L. Staykov, B. Steffen, F. Stephan, F. Stulle, H. Thom, K. Tiedtke, M. Tischer, S. Toleikis, R. Treusch, D. Trines, I. Tsakov, E. Vogel, T. Weiland, H. Weise, M. Wellhöfer, M. Wendt, I. Will, A. Winter, K. Wittenburg, W. Wurth, P. Yeates, V. Yurkov, I. Zagorodnov, and K. Zapfe, *Nat. Photon.* **1**, 336 (2007).
3. J. Chalupský, V. Hájková, V. Altapova, T. Burian, A. J. Gleeson, L. Juha, M. Jurek, H. Sinn, M. Störmer, R. Sobierajski, K. Tiedtke, S. Toleikis, T. Tschentscher, L. Vyšín, H. Wabnitz, and J. Gaudin, *Appl. Phys. Lett.* **95**, 031111 (2009).
4. P. Heimann, O. Krupin, W. F. Schlotter, J. Turner, J. Krzywinski, F. Sorgenfrei, M. Messerschmidt, D. Bernstein, J. Chalupský, V. Hájková, S. Hau-Riege, M. Holmes, L. Juha, N. Kelez, J. Lüning, D. Nordlund, M. F. Perea, A. Scherz, R. Soufli, W. Wurth, and M. Rowen, *Rev. Sci. Instrum.* **82**, 093104 (2011).
5. J. Chalupský, J. Krzywinski, L. Juha, V. Hájková, J. Cihelka, T. Burian, L. Vyšín, J. Gaudin, A. Gleeson, M. Jurek, A. R. Khorsand, D. Klinger, H. Wabnitz, R. Sobierajski, M. Störmer, K. Tiedtke, and S. Toleikis, *Opt. Express* **18**, 27836 (2010).
6. O. K. Ersoy, *Diffraction, Fourier Optics and Imaging* (Wiley, 2007).
7. H. J. W. M. Hoekstra, *Opt. Quantum Electron.* **29**, 157 (1997).
8. B. L. Henke, E. M. Gullikson, and J. C. Davis, *At. Data Nucl. Data Tables* **54**, 181 (1993).